IJST, Transactions of Civil Engineering, Vol. 37, No. C2, pp 203-218
Printed in The Islamic Republic of Iran, 2013

HAZARD MITIGATION AND EXTERNALLY FRP RETROFITTING OF RC BUILDINGS SUBJECTED TO NEAR-FAULT GROUND MOTIONS HAVING FORWARD DIRECTIVITY*

A. R. MORTEZAEI

Dept. of Civil Engineering, Engineering Faculty, Semnan Branch, Islamic Azad University, Semnan, I. R. of Iran
Email: a.mortezaei@semnaniau.ac.ir

Abstract– Ground motions in the near field of a rupturing fault differ from ordinary ground motions, as they contain a large energy, or "directivity" pulse. This pulse can cause considerable damage during an earthquake. Failures of modern engineered structures observed within the near-fault region in the recent earthquakes have revealed the vulnerability of existing RC buildings against pulse-type ground motions. This may be due to the fact that these modern structures had been designed primarily using the design spectra of available standards which was developed using stochastic processes with relatively long duration that characterizes more distant ground motions. Many recently designed and constructed buildings may therefore require strengthening in order to perform well when subjected to near-fault ground motions. This paper presents the results of a study of the response of typical existing RC buildings to near-fault ground motions and the potential improvements achievable after FRP retrofitting of the buildings. Results show that in case of near-fault records, they impose higher demands in comparison to far-fault records, though the maximum drift is generally concentrated at the middle story levels. It is demonstrated that strengthening with FRP is very effective in reducing drift demands for structures for a wide range of natural periods. The rehabilitated buildings possess an elastic stiffness 1.4 times that of the original buildings and have a total shear force capacity, 1.5 times that of the original buildings. The cumulative energy dissipation for rehabilitated specimens is 2.3 times that of the original building, on average.

Keywords– Forward directivity, near-fault ground motion, rehabilitation, FRP, dynamic analysis

1. INTRODUCTION

Impulsive type motions can cause considerable damage during an earthquake, especially to structures with natural periods close to those of the pulse. Near-fault effects can be broken down into three types depending on the pulses, i.e. whether they are of acceleration, velocity, or displacement type. The velocity pulse motion, sometimes referred to as "fling," represents the cumulative effect of almost all of the seismic radiation from the fault [1]. From a seismological perspective, the velocity pulse is more commonly found in earthquake records than are acceleration or displacement pulses. Although from an engineer's perspective, the velocity pulse is a better indicator of damage than the acceleration pulse, the damage potential is also dependent on the peak displacement during the pulse [2].

The displacement pulse without the high velocity pulse does not have a high damage potential because the structure has time to react to the displacements. After the 1971 San Fernando earthquake, engineers and seismologists realized the potential damage that may occur due to the effects of near-fault ground motions on structures. The damage observed during the 1994 Northridge, California, the 1995 Kobe, Japan, the 1999 Izmit, Turkey, the 2003 Bam, Iran, the 2008 Sichuan, China and the 2011 Tohoku, Japan earthquakes proved the engineers' hypothesis that structures located within the near-fault area suffered more severe damage than structures located outside of this zone. These earthquakes provided a

*Received by the editors August 17, 2011; Accepted November 20, 2012.

wealth of new information about the behaviour of engineered structures because the respective epicentres were in urban settings. Based on the data collected, building designers started studying the near-fault effects on buildings. Their research and findings led to the implementation of design factors in the 1997 Uniform Building Code [3] and 2000 International Building Code [4].

Although design codes and provisions introduce site-source and distance-dependent near-source factors, the effectiveness of constant amplification factors in providing adequate ductility levels to structures located in the proximity of fault zones is questionable [5]. This is because current design spectra were developed using stochastic processes with relatively long duration which characterizes more distant ground motions. On the other hand, failures of modern engineered structures observed within the near-fault region in recent earthquakes revealed the vulnerability of existing RC buildings against pulse-type ground motions.

Extensive investigations into the seismic performance of reinforced concrete frame buildings have been performed [6-8]. These studies showed at a local level that most of the damage is likely to occur in the beam-column joint panel zone and that the formation of soft-story mechanisms can greatly impair the global structural performance of the systems. A comprehensive overview of traditional seismic rehabilitation techniques was presented by FEMA-547 [9]. Conventional techniques which utilize braces, jacketing or infills, as well as more recent approaches including base isolation and supplemental damping devices, have been considered to strengthen the building and as such, improve its behaviour. In the past decade, an increased interest in the use of advanced non-metallic materials has been reported.

The objective of this research is to use the wealth of recent ground motion data to improve the understanding of the response of typical reinforced concrete buildings to pulse-type ground motions that result from forward-directivity effects, and also to discuss the feasibility and efficacy of a retrofitting intervention using FRP composite materials in order to upgrade a far-fault earthquake designed RC building to a near-fault one. In the following, firstly the seismic risk reduction and rehabilitation of existing buildings is described, followed by characteristics of near-fault ground motions, seismic response evaluation, proposed seismic retrofitting with FRP and shear walls, the results and conclusions drawn from the study.

2. NEAR-FAULT GROUND MOTIONS AND SEISMIC RISK REDUCTION

Rehabilitation, or seismic retrofit becomes necessary if it is shown, through a seismic performance evaluation, that the building does not meet the minimum requirements of the current building code, and that it may suffer severe damage or even collapse during a seismic event [8]. Once the potential losses in an existing building have been quantified through a detailed seismic evaluation, a decision must be made whether to (a) take no action; (b) do minimum repair and/or modifications; (c) retrofit; or (d) demolish the building and replace it with a new building. The decision on the course of action is usually complex as it involves many factors [10].

The selection of adequate rehabilitation strategies depends on the particular building in question. Some of the main factors affecting this selection are: (1) fundamental period of vibration; (2) actual strength; (3) initial stiffness; (4) deformability; (5) type of mechanism; (6) local site conditions; (7) level of safety required; and (8) level of seismic hazard. The application of fiber reinforced polymer (FRP) materials has opened an exciting new path for structural repair and strengthening. The prime material types that are useful as reinforcing fibbers for strengthening applications are glass, carbon and aramid. FRPs have very low self weight but high strength-to-weight ratio and do not exhibit any corrosion problems. This results in low maintenance costs. Such versatility may predict a rapid increase in their usage.

When a fault rupture propagates toward a site at a velocity close to that of the shear wave velocity, an accumulation of most of the energy of the seismic radiation of the fault can arrive at the site as a single

long-period pulse. This is called a directivity pulse [11]. The rupture is broken into sub-faults; beginning at the epicentre, the rupture propagates along the fault in the direction of the arrow toward Site A (Fig. 1). Because the velocity of the shear waves is close to the rupture velocity, the energy of the forward direction arrives within a short time period. Forward directivity effects only occur when the rupture propagates toward the site, and the direction of slip on the fault is aligned with the site. Not all near-fault locations will experience forward rupture directivity effects in a given event. As can be seen from the model, Site B (Fig. 1) will experience a lengthening of the time inbetween the arrivals of the waves; thus the record at Site B will have a long duration but not a velocity pulse [12].

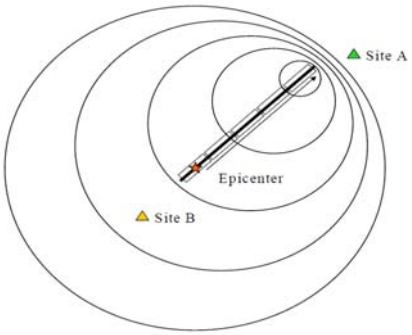

Fig. 1. Zones of directivity and directivity pulse accumulates as rupture propagates to right [12]

The velocity and displacement time histories of typical near-fault ground motions having forward-directivity (Rinaldi record of 1994 Northridge earthquake) effects are compared to those of ordinary far-fault motion (Taft record of 1952 Kern County earthquake) in Fig. 2. High-velocity pulses are quite distinctive for Rinaldi; such pulses do not exist in a typical far-fault ground motion like Taft.

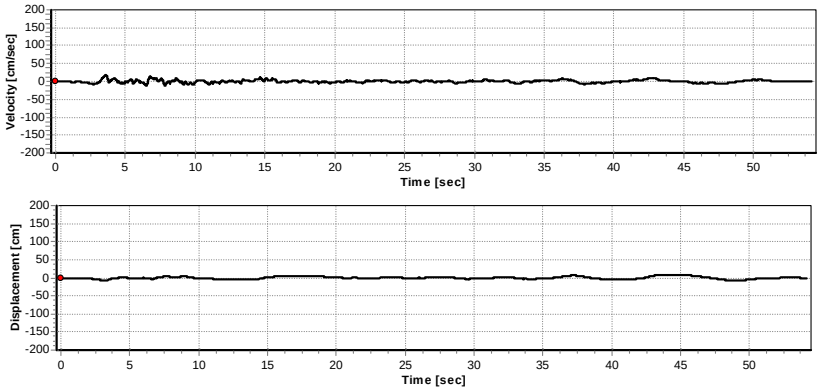

(a) Taft record of 1952 Kern County earthquake

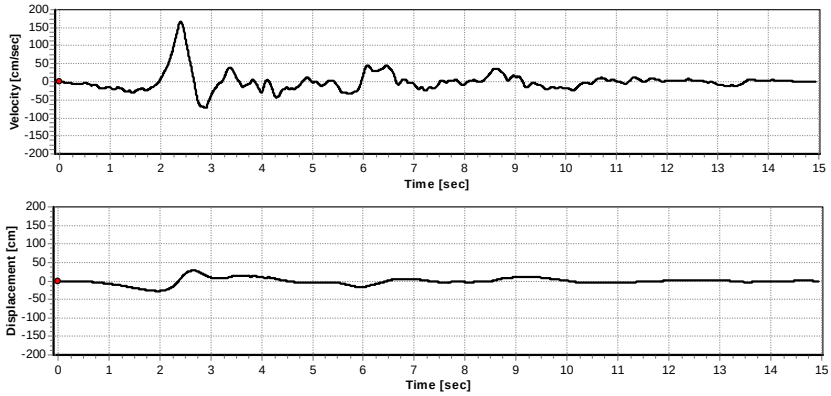

(b) Rinaldi record of 1994 Northridge earthquake

Fig. 2. Typical velocity and displacement time histories of (a) far-fault, (b) near-fault (forward-directivity) ground motions

3. DESCRIPTION OF BUILDINGS USED FOR EVALUATION

To select an appropriate retrofitting method, an accurate evaluation of both the seismic performance and the condition of an existing structure is necessary. Based on this evaluation, engineers can choose the most effective retrofit among the various intervention techniques and optimize the improvement in seismic performance for an existing structure. Seismic deficiencies should first be identified through a seismic evaluation of the structure.

Six existing reinforced concrete special moment-resisting frame buildings of 3, 6, 10, 14, 16 and 19 stories were selected as representative case studies to evaluate their seismic demands when subjected to near-fault ground motions with forward directivity, and to compare their respective responses to typical far-fault ground motions. Buildings with three, six and ten stories possess a moment-resisting frame system and the buildings with fourteen, sixteen and nineteen stories, a wall-frame system. The rectangular plan of all buildings measures 30 m × 25 m. The floor plans of the buildings with columns and shear walls locations are shown in Fig. 3. The buildings are assumed to be fixed at the base with a damping ratio of 5% in all modes, and the floors as rigid diaphragms with infinite in-plane stiffness. The sections of structural elements are square and rectangular and their dimensions are changed at different stories. The slab thickness is 100 mm. For the sake of clarity, the column and beam dimensions and reinforcement of the 10-story building are provided in Tables 1 and 2. Story heights of buildings are assumed to be constant with the exception of the ground story. The modulus of elasticity (Young's modulus) E = 30 kN/mm^2, Poisson's ratio ν = 0.20 and the mass density ρ = 24 kN/m^3 are assumed in all models. The uniaxial strength for nonlinear modelling of the concrete is considered to be 35 MPa. The rebar is modeled as steel with yield strength of 400 MPa and an ultimate strength of 600 MPa. Permanent and imposed loads are assumed to be: dead load of story level, 5.5 KPa; dead load of roof, 6 KPa; dead load of partitions, 1 KPa; dead load of external walls, 2.5 KPa; live load of story levels, 2 KPa; and live load of roof, 1.5 KPa.

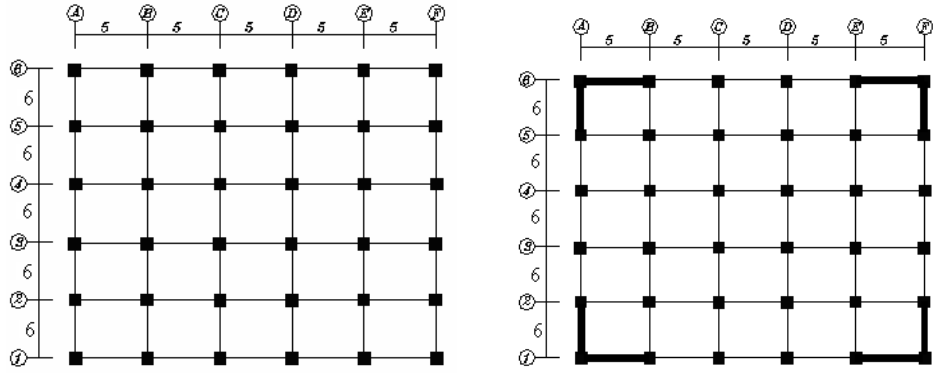

(a) (b)

Fig. 3. Structural configuration of (a) 3, 6 and 10 story; and (b) 14, 16 and 19 story buildings (units: meter)

Table 1. Dimensions and amount of reinforcement of columns and shear walls in the 10-story building

Building	Story	Corner column		Perimeter column		Internal column		Shear wall
		Dim. (cm)	Reo. (mm^2)	Dim. (cm)	Reo. (mm^2)	Dim. (cm)	Reo. (mm^2)	Thickness (cm)
10 story	1	60×60	2100	60×60	1880	60×60	1930	-
	2	60×60	1200	60×60	1200	60×60	1200	-
	3	60×60	1200	60×60	1200	60×60	1200	-
	4	60×60	1200	60×60	1200	60×60	1200	-
	5	50×50	910	50×50	1335	50×50	950	-
	6	50×50	840	50×50	910	50×50	840	-
	7	50×50	840	50×50	900	50×50	840	-
	8	40×40	775	40×40	1070	40×40	840	-
	9	40×40	600	40×40	880	40×40	600	-
	10	40×40	600	40×40	880	40×40	600	-

Table 2. Dimensions and amount of reinforcement of beams in 10-story building

Story	Beams of external frames						Beams of internal frames					
	Type 4			Type 3			Type 2			Type 1		
	Dim. (cm) h.×w.	Reo. (mm^2) Bot.	Top	Dim. (cm) h.×w.	Reo. (mm^2) Bot.	Top	Dim. (cm) h.×w.	Reo. (mm^2) Bot.	Top	Dim. (cm) h.×w.	Reo. (mm^2) Bot.	Top
1	60×50	1316	1664	60×50	1108	1583	60×50	1176	1670	60×50	1104	1593
2	60×50	1685	2071	60×50	1488	1972	60×50	1532	2093	60×50	1484	1981
3	60×50	1728	2141	60×50	1566	2054	60×50	1568	2176	60×50	1562	2059
4	60×50	1764	2181	60×50	1564	2043	60×50	1600	2223	60×50	1557	2055
5	50×45	1484	1931	50×45	1276	1823	50×45	1298	1965	50×45	1270	1835
6	50×45	1393	1860	50×45	1221	1770	50×45	1203	1903	50×45	1214	1778
7	50×45	1287	1737	50×45	1076	1607	50×45	1103	1779	50×45	1066	1625
8	40×40	947	1424	40×40	711	1334	40×40	738	1449	40×40	702	1352
9	40×40	665	1157	40×40	529	1100	40×40	570	1190	40×40	533	1110
10	40×40	495	760	40×40	473	727	40×40	502	773	40×40	492	757

4. GROUND MOTION DATABASE

The ground motion database compiled for nonlinear time-history (NTH) analyses constitutes a representative number of far-fault and near-fault ground motions from a variety of tectonic environments. A total of 14 records were selected to cover a range of frequency content, duration and amplitude. Near-fault records were chosen so as to consider the presence of forward-directivity effects. Hence the assembled database can be investigated in two sub-data sets. The first set contains seven ordinary far-fault ground motions recorded within 90 km of the causative fault plane from earthquakes in the magnitude (M_W) range of 6.5 to 7.4. The second set includes seven near-fault ground motions characterized with forward-directivity effect. These records come from earthquakes having a magnitude (M_W) range of 6.5 to 7.4, and recorded at closest fault distance of 0.0 to 10 km. Information pertinent to the ground motion data sets, including station, component of earthquake and peak ground acceleration (PGA), peak ground velocity (PGV), and peak ground displacement (PGD), are presented in Tables 3 and 4 and their elastic acceleration response spectra are shown in Fig. 4.

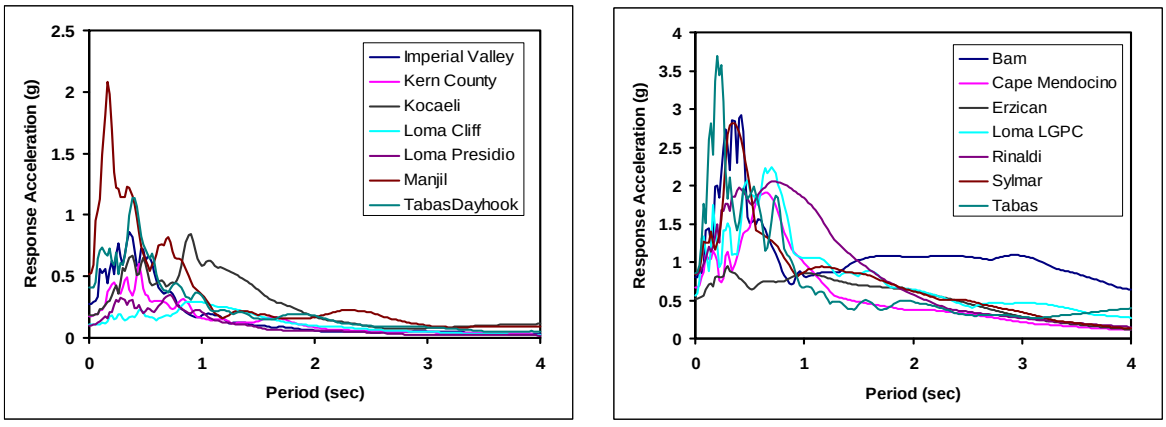

(a) (b)

Fig. 4. Elastic acceleration response spectra of (a) far-field and (b) near-fault ground motion recordings used in the evaluation of each building

Table 3. Far-fault ground motion database

NO.	Earthquake	Year	Station	Comp.	M_w	Dis. (km)	PGA (g)	PGV (cm/s)	PGD (cm)
1	Kern County	1952	Taft	111	7.4	81	0.17	17.47	8.83
2	Tabas	1978	Dayhook	TR	7.4	107	0.4	26.17	9.1
3	Imperial Valley	1979	Calexico	225	6.5	90.6	0.27	21.23	8.98
4	Loma Prieta	1989	Presidio	000	6.9	83.1	0.099	12.91	4.32
5	Loma Prieta	1989	Cliff House	90	6.9	84.4	0.107	19.78	5.06
6	Manjil	1990	Abbar	L	7.3	74	0.51	42.46	14.92
7	Kocaeli	1999	Ambarli	90	7.4	78.9	0.18	33.22	25.84

Table 4. Near-fault ground motion database

NO.	Earthquake	Year	Station	Comp.	M_w	Dis. (km)	PGA (g)	PGV (cm/s)	PGD (cm)
1	Tabas	1978	Tabas	TR	7.4	3	0.85	121.22	95.06
2	Loma Prieta	1989	LGPC	00	7.0	1.3	0.56	94.71	41.13
3	Cape Mendocino	1992	Petrolia	90	7.1	9.5	0.66	89.68	28.99
4	Erzincan	1992	Erzincan	NS	6.9	2	0.51	83.95	27.66
5	Northridge	1994	Rinaldi	228	6.7	7.1	0.83	166.03	28.15
6	Northridge	1994	Sylmar	360	6.7	6.4	0.84	129.3	31.92
7	Bam	2003	Bam	L1	6.5	7	1.09	131.26	89.24

* Data source: PEER (http://peer.berkeley.edu/smcat)

Ground motions employed in this paper were scaled such that the spectrum of each record matches the Standard NO. 2800-05 [13] design spectrum with minimum error in the period range of 0.6sec to 4.0sec. In this study, a data processing technique proposed in Iwan et al. [14] and refined in Iwan and Chen [15] was also utilized to recover the long period components from near-fault accelerograms. This process has been extensively elaborated in Boore [16] and Boore et al. [17].

5. FINITE ELEMENT PROGRAM

Nonlinear dynamic analyses were performed using a program previously developed by the author [18]. This program can be used to predict the nonlinear behaviour of any plain, reinforced or prestressed concrete structure that is composed of thin plate members with plane stress conditions. This includes beams, slabs, shells, girders, shear walls, or any combination of these structural elements.

Two types of element modeling, i.e. Phenomenological and Macroscopic, were used for analyzing the selected RC structures. Phenomenological models, which are more practical, were utilized for general assessment of buildings. Macroscopic model attempts to represent behavior down to the “fiber” level. These models have the advantage of automatically including some aspects of complex behavior, such as axial-flexural interaction, crack pattern and so on. An explanation about macroscopic models used for detailed assessment of RC buildings is mentioned below.

6. CONCRETE PROPERTIES

Concrete behaves differently under different types and combinations of stress conditions due to the progressive micro-cracking at the interface between the mortar and the aggregates (transition zone). The propagation of these cracks under the applied loads contributes to the nonlinear behavior of the concrete. There are many existing concrete constitutive models to simulate cyclic loading effects. The model accepted for this research is a computational constitutive model for concrete subjected to large strains. As shown in Fig. 5a, the uniaxial stress-strain curve of concrete adopted in this study comprises two parts. The ascending branch up to the peak compressive strength is represented by the equation proposed by

Ashour and Morley [19]:

$$\sigma = \frac{E_0 \varepsilon}{1 + \left(\frac{E_0}{E_{sc}} - 2\right)\left(\frac{\varepsilon}{\varepsilon_{max}}\right) + \left(\frac{\varepsilon}{\varepsilon_{max}}\right)^2} \quad (1)$$

where E_0 is the initial modulus of elasticity of the concrete, E_{sc} is the secant modulus of the concrete at the peak stress, σ is stress, ε is strain and ε_{max} is the strain at peak stress. The descending, or the strain-softening branch is idealized by the Bazant et al. model [20]:

$$\sigma = \sigma_c \left(\frac{\varepsilon}{\varepsilon_{max}}\right) \exp\left(1 - \varepsilon / \varepsilon_{max}\right) \quad (2)$$

where σ_c is compressive strength of the concrete. For uniaxially loaded concrete, σ_c is equal to f'_c.
Regarding the stress–strain relationships for cyclic loading, it is important to distinguish between the unloading paths before and after the compression strength (Fig. 5b) is exceeded. In the first case, the unloading path is a straight line defined by the elastic modulus E_0 and tensile stresses are still possible. In the second case, the unloading path doesn't reach the tensile region. After exceeding the maximum tensile strength, cracks occur perpendicular to the principal stress direction. Based on a smeared crack model a smeared crack width is then calculated.

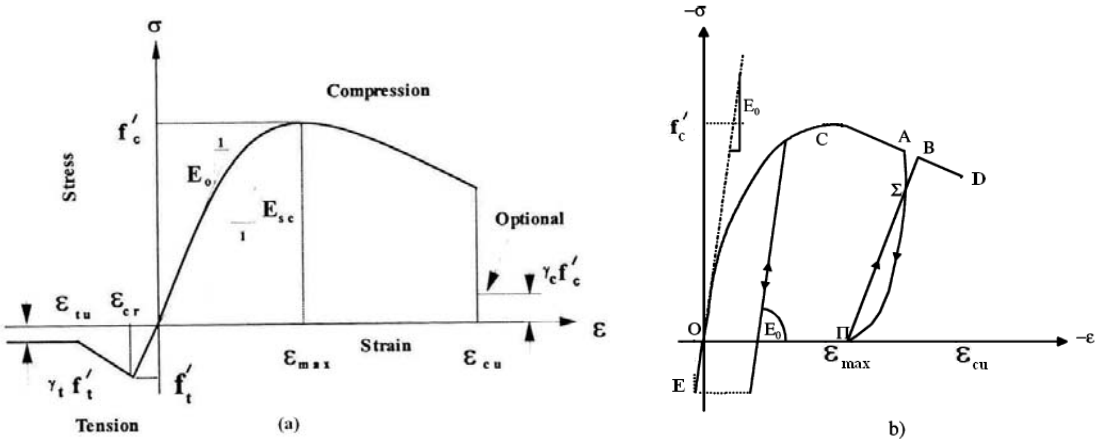

Fig. 5. The stress–strain relationship of concrete for (a) monotonic loading; (b) cyclic loading

7. FINITE ELEMENT FORMULATION AND DYNAMIC ANALYSIS

In this paper, three-node constant strain triangular elements were used with six degrees of freedom (DOF) and four-node plane stress rectangular elements with eight DOF to model concrete with distributed reinforcement, using two-node truss bar elements with four DOF to model discrete reinforcement.

For the analysis of nonlinear dynamic response of structures, the dynamic analyses were done using the increment form. Firstly, the equation of dynamic equilibrium is expressed in terms of the increment form of nodal displacement by using the step by step integration method. Then the equation is related to the elasto-plastic constitutive laws, the compatibility and equilibrium conditions for analysis to give the relationship of dynamic behavior and the nodal displacement vector expressed in terms of the external forces and the plastic deformation. At any instant of time, for a finite time step, Δt, the equation of dynamic equilibrium can be written as:

$$[M]\{\Delta\ddot{u}\} + [C]\{\Delta\dot{u}\} + [K]\{\Delta u\} = -[M]\{I\}\Delta\ddot{u}_g \quad (3)$$

Where [M] and [C] are the mass matrix and damping matrix, [K] is the stiffness matrix for assembled structure, $\{\Delta\ddot{u}\}$, $\{\Delta\dot{u}\}$ and $\{\Delta u\}$ are the increment vectors of acceleration, velocity and displacement, respectively, $\Delta\ddot{u}_g$ is the increment of ground acceleration and $\{I\}$ is a unit vetor.

8. VERIFICATION OF FINITE ELEMENT PROGRAM

The capability and accuracy of the finite element program and analytical models in predicting the nonlinear response of FRP strengthened RC buildings were verified along with a comparison between the analytical and corresponding experimental results in two levels, i.e. component level and element level. For the sake of brevity, these results were not provided in the paper. For example, in the component level, Colomb et al. [21] test data were used. Colomb et al. [21] tested eight columns under a constant compression load combined with a horizontal quasi-static cyclic load. Details of test specimens and the configuration of FRP sheets can be found in Ref. [21]. At the start of the test, axial load was applied to the column specimen after which the column was subjected to gradually increasing lateral displacement cycles. The column, sheets, and supports were modeled as volumes. In the model, rebar shares the same nodes at the points that it intersects with the shear stirrups. The meshing of the reinforcement is a special case compared to the volumes. No meshing of the reinforcement was needed because individual elements were created in the modeling through the nodes created by the mesh of the concrete volume.

The goal of the comparison between the finite element model and the experimental work is to ensure that the elements, material properties, real constants and convergence criteria are adequate to model the response of the member. The shear force-lateral displacement hysteresis curve of analytical model and experimental work is shown in Fig. 6. The results indicate that finite element program provide reasonable results in component level and can be used to approximate the nonlinear behavior of FRP strengthened RC columns under a dynamic load.

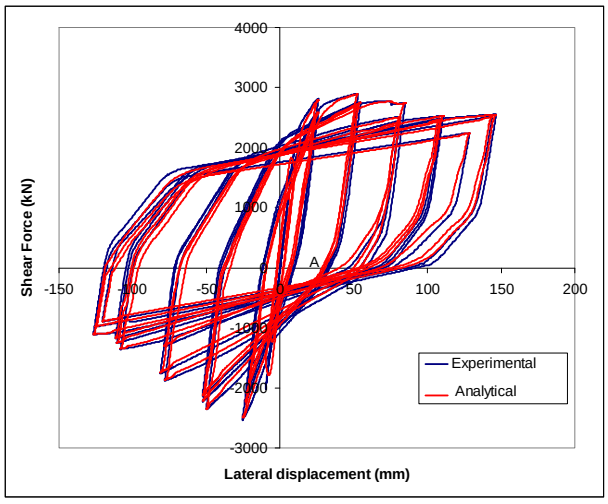

Fig. 6. The shear force-lateral displacement hysteresis curve of analytical model and experimental work 3-story building

9. SEISMIC RESPONSE EVALUATION OF BUILDINGS

In total, 168 nonlinear time history (NTH) analyses were conducted on the six buildings. Inter-story drift ratio (IDR), defined as the relative displacement between two consecutive story levels, displacements at different story levels, base shear force, base bending moment and shear forces at different story levels are used as the primary measure of seismic demand. Additional demand measures, such as component and story ductility were also investigated. In general, there is a reasonable correlation between the inter-story drift demands and component/story-level ductility demands; hence these results are not included here. The

peak inter-story drift profiles obtained from NTH analyses of the buildings subjected to the two sets of ground motions (i.e., far-fault motions, near-fault motions with forward directivity) are presented in Fig. 7.

3-story building

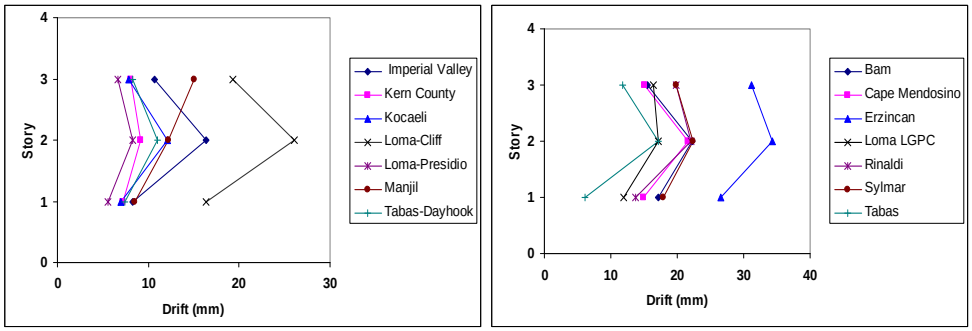

(a) (b)

6-story building

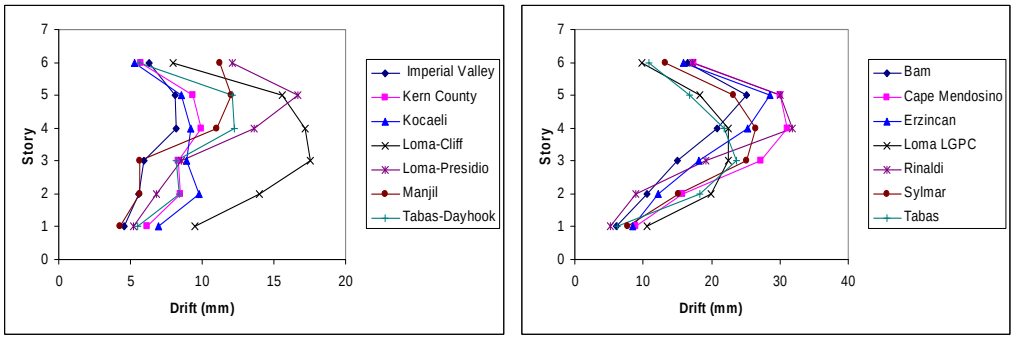

(a) (b)

10-story building

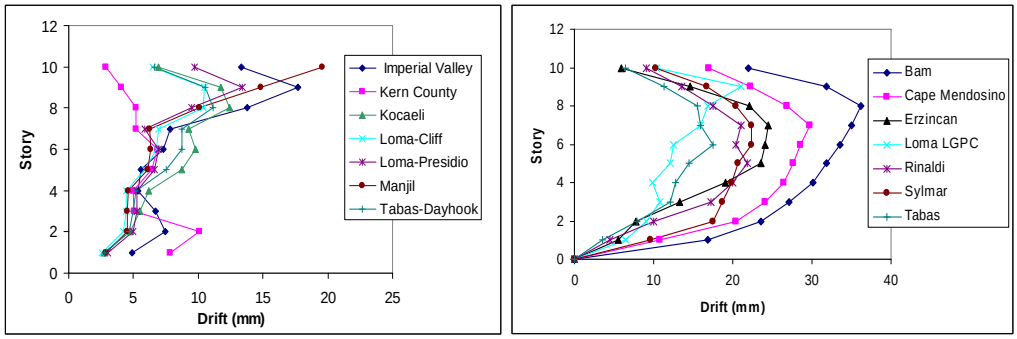

(a) (b)

14-story building

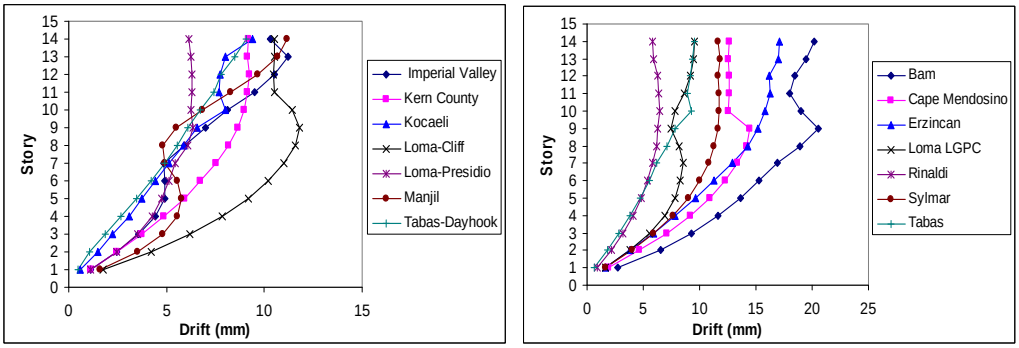

(a) (b)

16-story building

Fig. 7. Maximum inter-story drift for each building subjected to (a) far-fault earthquakes, (b) near-fault earthquakes with forward directivity

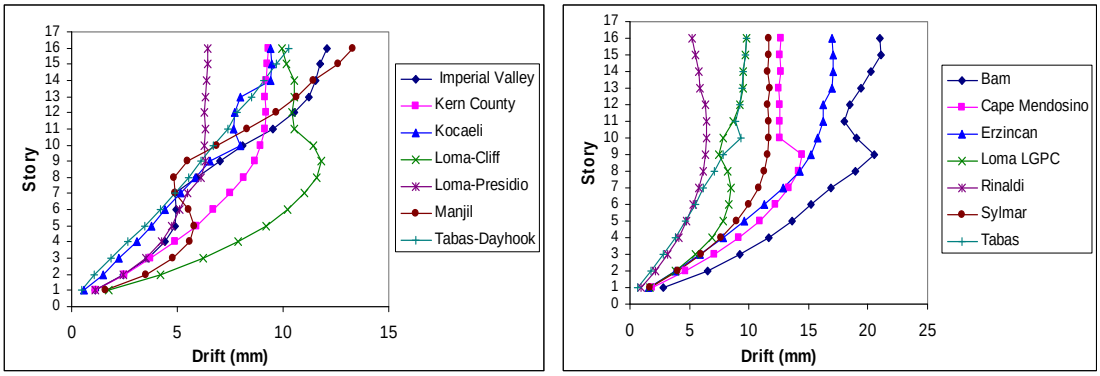

(a) (b)

19-story building

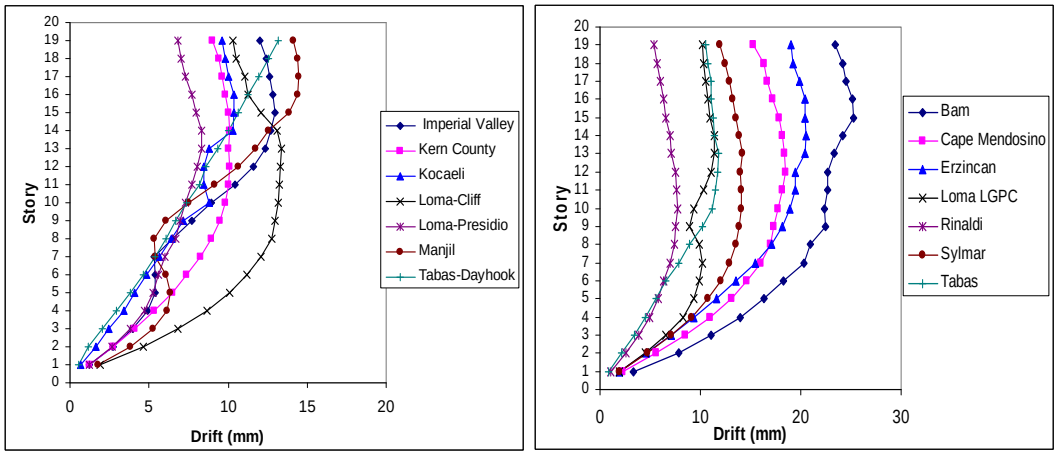

(a) (b)

Fig. 7. (Continued)

For the 3-story building, far-fault motions produce nearly uniform inter-story drift demands for most records, with the exception of the Loma-Cliff record. In case of near-fault records, they impose higher demands in comparison to far-fault records, though the maximum drift is generally concentrated at the middle story levels. The largest demand was caused by the Erzincan record, which produced 34.4 mm inter-story drift at the second story. For the 6-story building, the maximum story demand for far-fault records is observed to be either at the second or third story levels and depends on the frequency content of the motion. For near-fault records, the demands at the upper levels are much higher. Of the entire data set, the Rinaldi record generated the highest demand (31.8 mm inter-story drift) at the third story. For the 10-story building, the Bam record generated the highest demand (38.71 mm inter-story drift) at the eighth story level. Higher-mode effects are predominant in many of the near-fault records causing a shift in demand from the lower to upper stories.

For the 14-story building, the maximum story demand for far-fault records is observed to be either at the 7th or 8th story levels and depends on the frequency content of the motion. Though similar observations hold for near-fault records, the demands at the upper levels are much higher. Of the entire data set, the Bam record generated the highest demand (20.56 mm inter-story drift) at the 9th story. Similar results were observed for 16- and 19-story buildings. In both buildings, the Bam record generated the highest demand (21.1 mm and 25.32 mm inter-story drift for 16- and 19-story buildings, respectively).

The variation in story demand for the far-fault records is less significant. While higher-mode effects are expected to contribute to the response of the 6- and 10-story buildings, the response of the 3-story building demonstrates that even for low rise buildings, higher-mode effects could be significant.

10. SEISMIC RETROFITTING WITH FIBER REINFORCED POLYMER

Fiber reinforced polymer (FRP) materials are composites consisting of high strength fibers embedded in a polymeric resin. Fibers in an FRP composite are the load-carrying elements, while the resin maintains the fibers' alignment and protects them against the environment and possible damage. Among commercially available fibers, those made from carbon exhibit the highest strength and stiffness when compared with steel. The type of fiber is selected based on mechanical properties and durability requirements, while the type of resin depends upon environmental and constructability needs [22].

Recent research and development efforts have led to many applications of composite materials for strengthening existing reinforced concrete structures. Ease of construction and broader applications have made fiber composite sheets a more popular choice than plates. While plates are appropriate for flat surfaces and beams, sheets can be used on round (such as columns) and larger (such as walls) surfaces more efficiently and effectively. The primary load-carrying element within a composite is the fiber. Consequently, the fiber has a strong influence on the mechanical characteristics of the composite such as strength and elastic modulus. The resin provides a mechanism for the transfer of load among the fibers [23]. It also protects the fibers from abrasion and other environmental and chemical effects. The fibers can be oriented in a single direction (unidirectional) or several directions, to optimize the performance of the composite. Fiber strengthening technique (by wrapping the element with fiber composite sheets) is a relatively simple process. As a result, the above-mentioned analysed RC structures were loaded by near-fault earthquake loads, up to the development of a clear plastic collapse mechanism. After that, these structures were retrofitted. The main aim of the retrofitting system design was to change the failure mode from a column-type to a beam-type collapse mechanism, forcing plastic hinges to form in the beams. The mechanical properties of the FRP composite used for this rehabilitation are: Tensile strength=880MPa, Young modulus=165Gpa and Ultimate strain=1.1%. RC elements were reinforced by two layers of carbon FRP of 100 mm in width, 100 mm apart.

The analytical results showed that typical RC buildings can be subjected to large displacement demands at the arrival of the velocity pulse, which require the structure to dissipate considerable input energy in a single or relatively few plastic cycles. This demand will impact those structures with limited ductility capacity. In contrast, far-fault motions build input energy more gradually, and the displacement demands are on average lower than the demands in near-fault records. Dynamic analysis demonstrated the migration of demands from lower to upper stories under the near-fault ground motions. Therefore, according to the nonlinear finite element analysis, a few plastic hinges had developed in the panel zone and columns at higher levels.

For all of the near-fault earthquakes investigated in this study, the severity of the demand is controlled by nonlinear finite element analysis. Results show that near-fault motions characterized by forward directivity effects are potentially more damaging in the upper one-third of buildings (Figs. 8 and 9). Therefore, in this paper, all panel zones and the tops and bottoms of columns were strengthened with FRP sheets.

11. RESULTS OF ANALYSES

All buildings were analysed under the near-fault ground motions. The shear strength of a column tended to degrade faster than its flexural strength with cycling of the lateral load. For beam members, flexural cracks were observed. In some cases, flexural cracks occurred on the bottom face of the beams. Shear cracking was observed in shear walls and beam-column joints during the near-fault earthquakes.

For the sake of clarity, results of the demands on the interior frame of the 10-story building experiencing the largest demand among each ground motion category are presented. For the 10-story

building, plastic hinges occurred at the upper levels of the building (Fig. 8). Due to the significant contribution of joint failures to the collapse of buildings during earthquakes, it is necessary to rehabilitate the joints. These locations were selected for rehabilitation with FRP. On average, the rehabilitated buildings had a total shear force capacity *V*, 1.5 times that of the original buildings as shown in Fig. 10. Application of FRP increased the stiffness and ductility of the rehabilitated buildings. The rehabilitated buildings had an elastic stiffness which was 1.4 times that of the original building.

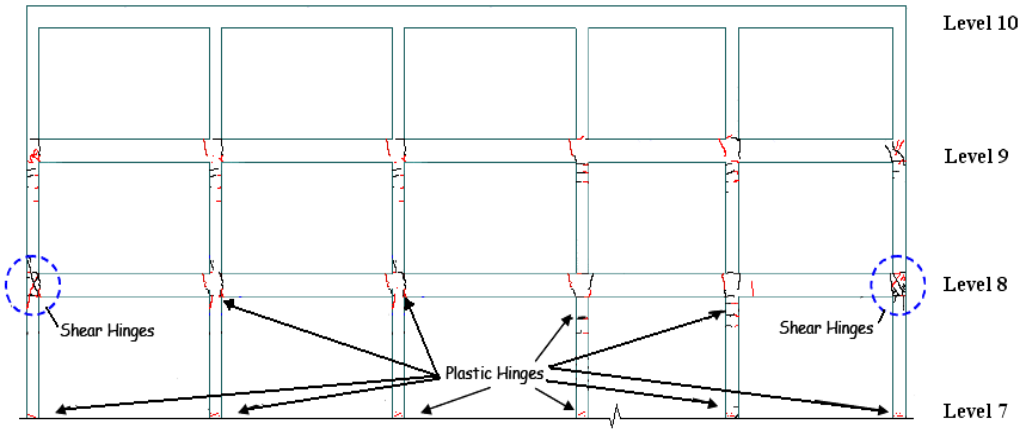

Fig. 8. Formation of plastic hinge in upper levels of 10-story RC buildings

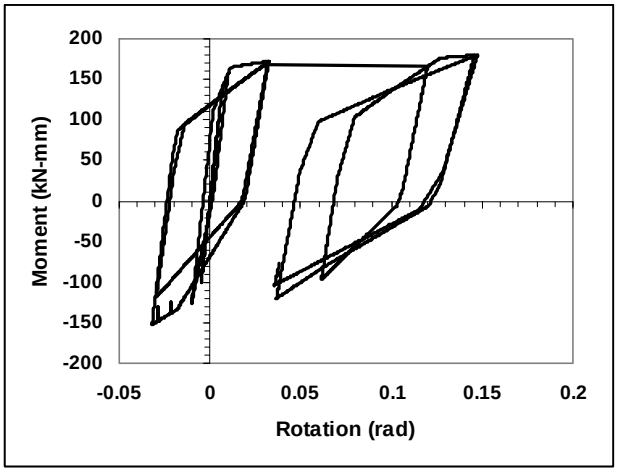

Fig. 9. Cyclic behaviour of a critical column under the near-fault record

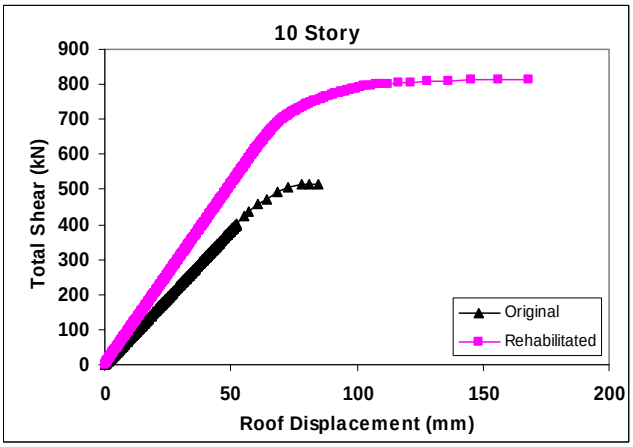

Fig. 10. Relationship between total shear and roof displacement in 10-story building

To compare the behaviour of the results, backbone curves were plotted (Fig. 11). The backbone curves were generated for energy dissipation-drift relationships. The procedure to develop backbone curves was adopted from FEMA 356 [24]. FEMA 356 states that: "The backbone curve shall be constructed as follows: (1) A smooth 'backbone' curve shall be drawn through the intersection of the first cycle curve for the i-th deformation step with the second cycle curve of the i-th deformation step. (2) The backbone curve so derived shall be approximated by a series of linear segments, drawn to form a multi-segmented curve." Figure 10 shows the energy dissipation curves for the original and rehabilitated buildings. The cumulative energy dissipation for rehabilitated specimens was 2.3 times that of the original building, on average. This demonstrates that the energy dissipation capacity of the frames increased when they were rehabilitated using FRP. A comparison of the results of the 3-, 6- and 10-story analyses shows that the effect of FRP rehabilitation in increasing the story shear capacity is more significant for the high-rise building than for the low-rise building.

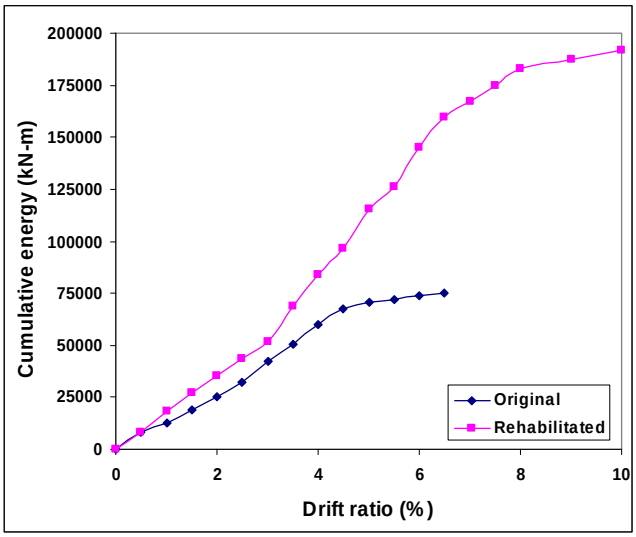

Fig. 11. Energy dissipation curves for original and rehabilitated buildings

12. BUILDINGS WITH SHEAR WALL

In earthquake resistant design, shear walls are common lateral load resistance systems found in many reinforced concrete structures. Since the 1950s, shear walls have been accepted as effective alternatives to moment resistant frames for providing the main earthquake resistance mechanism in the seismic design of concrete structures. The results of nonlinear dynamic analyses show that, for wall-frame system buildings, which are strengthened by shear walls, the maximum drift demands are reduced. The analyses show that some cracks have occurred in the walls at contra-flexure point of buildings.

Many different methods of seismic strengthening and repair of shear wall structures have been developed and tested in the last thirty years. These techniques include the strengthening of existing shear walls by the application of shotcrete or ferrocement, filling in openings with reinforced concrete and so on [25]. Research studies have shown that the concrete jacketing of a damaged shear wall can restore the gravity load carrying capacity of the wall, but is not as effective when the objective is to restore the lateral stiffness of the structure. For the purpose of strengthening, an alternative upgrade is the addition of steel bracings to the shear walls. Although this method is effective in recovering and enhancing the lateral stiffness of damaged and undamaged shear walls, it is architecturally unappealing since it changes the exterior and/or interior layout of the structure, and results in a significant reduction of the building's usable space. It may also add significant weight to the structure and thus alter the magnitude and

distribution of the seismic loads. Recently, applications of composite materials have been introduced as effective alternatives to conventional techniques for the retrofit and repair of RC shear walls.

For modeling of the shear wall, three-node constant strain triangular elements was used with six degrees of freedom (DOF) and four-node plane stress rectangular elements with eight DOF to model concrete with distributed reinforcement, and two-node truss bar elements with four DOF was used to model discrete reinforcement. Different concrete material types with different percentages of distributed horizontal and vertical reinforcement were used to represent the various wall regions. To investigate the flexural hinging near the base of the walls and floor levels, a refined mesh was used over the lower half of the walls. Typically 20 (approximately square) rectangular elements were used over the wall length for the lower portion of the wall. The total mesh for a typical wall consisted of approximately 2000 elements.

The repair by FRP sheets results in an increase of the load-carrying capacity compared to that of the original wall-frame building. The analytical results conclude that the application of externally bonded carbon fiber sheets is an effective seismic strengthening and repair procedure for reinforced concrete shear walls. The carbon fiber repair system can be used to recover the initial elastic stiffness and to increase the yield load and ultimate flexural capacity of seismically damaged walls. In strengthening applications, the carbon fiber sheets can be used to increase the pre-cracked stiffness, the secant stiffness at yield and the cracking load, the yield load and the ultimate flexural capacity of undamaged walls.

13. CONCLUSION

This paper explores FRP strengthening technique for RC buildings subjected to near-fault earthquakes. Many reinforced concrete (RC) frame structures designed according to the current codes are susceptible to abrupt strength deterioration once the shear capacity of the columns is reached. Fiber composites are used to increase the shear strength of existing RC columns and beams by wrapping or partially wrapping the members. Increasing the shear strength can alter the failure mode to a more ductile mode with higher energy dissipation and interstory drift ratio capacities. In case of near-fault records, they impose higher demands in comparison to far-fault records, though the maximum drift is generally concentrated at the middle story levels. The objective of this study was to analytically evaluate the effect of fiber reinforced polymer (FRP) rehabilitation on the seismic performance of six existing RC buildings when subjected to near-fault ground motion records. The study investigates the effect of the FRP strengthening on the capacities of the structures with respect to maximum inter-story drift ratio, maximum shear story and maximum energy dissipation. It was found that the maximum inter-story drift value decreases with the FRP strengthening, which leads to a more ductile behaviour.

In general, columns are critical elements in any structural system and their performance during a seismic event can dominate the overall outcome of the structure. The rehabilitated buildings possess an elastic stiffness 1.4 times that of the original buildings and have a total shear force capacity 1.5 times that of the original buildings. The cumulative energy dissipation for rehabilitated specimens is 2.3 times that of the original building, on average.

REFERENCES

1. Somerville, P. (1997). The characteristics and quantification of near-fault ground motion. *Proceedings of the FHWA/NCEER Workshop on the National Representation of Seismic Ground Motion for New and Existing Highway Facilities*. Burlingame, California, May 1997.
2. Hall, J. F., Heaton, T. H., Halling, M. W. & Wald, D. J. (1995). Near-source ground motion and its effects on flexible buildings. *Earthquake Spectra*, Vol. 11, pp. 569-605.
3. International Conference of Building Officials, (1997). *Uniform building code*, Whitter, California.

4. International Conference of Building Officials, (2000). *International building code*. Whitter, California.
5. Mortezaei, A., Ronagh, H. R., Kheyroddin, A. & Ghodrati Amiri, G. (2011). Effectiveness of modified pushover analysis procedure for the estimation of seismic demands of buildings subjected to near-fault earthquakes having forward directivity. *The Structural Design of Tall and Special Buildings*, Vol. 20, No. 6, pp. 679-699.
6. Eshghi, S. & Zanjanizadeh, V. (2008). Retrofit of slender square reinforced concrete columns with glass fiber-reinforced polymer for seismic resistance. *Iranian Journal of Science and Technology. Transaction B: Engineering*, Vol. 32, No. B5, pp. 437-450.
7. Kheyroddin, A. & Mortezaei, A. (2008). The effect of element size and plastic hinge characteristics on nonlinear analysis of RC frames. *Iranian Journal of Science & Technology, Transaction B, Engineering*, Vol. 32, No. B5, pp. 451-470.
8. Mortezaei, A., Ronagh, H. R. & Kheyroddin, A. (2010). Seismic evaluation of FRP strengthened RC buildings subjected to near-fault ground motions having fling step. *Composite Structures*, Vol. 92, No. 5, pp. 1200-1211.
9. Techniques for the Seismic Rehabilitation of Existing Buildings, (2006). FEMA 547.
10. Esfahani, A. D., Mostofinejad, D., Mahini, S., Ronagh, H. R. (2011). Numerical investigation on the behavior of FRP-retrofitted RC exterior beam-column joints under cyclic loads. *Iranian Journal of Science and Technology. Transactions of Civil Engineering*, Vol. 35, No. C1, pp. 35-50.
11. Somerville, P. (2000). Characterization of near field ground motions. U.S.-Japan Workshop: Effects of Near-Field Earthquake Shaking, San Francisco.
12. Orozco, G. & Ashford, S. A. (2002). Effects of large pulses on reinforced concrete bridge columns. Pacific Earthquake Engineering Research Center, PEER Report 2002/23, College of Engineering, University of California, Berkely.
13. Iranian Code of Practice for Seismic Resistant Design of Buildings. (2005). Standard NO. 2800-05, Building and Housing Research Center.
14. Iwan, W. D., Moser, M. A. & Peng, C. Y. (1985). Some observations on strong-motion earthquake measurements using a digital accelerograph. *Bulletin of the Seismological Society of America*, Vol. 75, pp. 1225–1246.
15. Iwan, W. D. & Chen, X. D. (1994). Important near-field ground motion data from the Landers earthquake. *Proceedings of the 10th European Conference on Earthquake Engineering*, Vienna, Austria.
16. Boore, D. (2001). Effect of baseline correction on displacements and response spectra for several recordings of the 1999 Chi-Chi, Taiwan, earthquake. *Bulletin of the Seismological Society of America*, Vol. 91, No. 5, pp. 1199–1211.
17. Boore, D., Stephens, C. D. & Joyner, W. B. (2002). Comments on baseline correction of digital strong motion data: Examples from the 1999 Hector Mine California earthquake. *Bulletin of the Seismological Society of America*, Vol. 92, No. 4, pp. 1543–1560.
18. Mortezaei, A. (2009). *A program for three-dimensional nonlinear dynamic analysis of reinforced concrete buildings*. School of Civil Engineering, The University of Queensland, Brisbane, Queensland.
19. Ashour, A. F. & Morley, C. T. (1993). Three-dimensional nonlinear finite element modeling of reinforced concrete structures. *Finite Elements in Analysis and Design*, Vol. 15, pp. 43-55.
20. Bazant, Z. P., Belytschko, T., Yul-Woong, H. & Ta-Peng, C. (1986). Strain-softening materials and finite-element solutions. *Computers & Structures*, Vol. 23, pp. 163-180.
21. Colomb, F., Tobbi, H., Ferrier, E. & Hamelin, P. (2008). Seismic retrofit of reinforced concrete short columns by CFRP materials. *Composite Structures*, Vol. 82, No. 4, 475-487.
22. Kheyroddin, A., Naderpour, H., Amiri, G. G. & Vaez, S. R. H. (2011). Influence of carbon fiber reinforced polymers on upgrading shear behaviour of RC coupling beams. *Iranian Journal of Science and Technology. Transactions of Civil Engineering*, Vol. 35, No. C2, pp. 155-169.

23. Li, W., Li, Q., Jiang, W. & Jiang, L. (2011). Seismic performance of composite reinforced concrete and steel moment frame structures - state-of-the-art. *Composites: Part B*, Vol. 42, No. 5, pp. 190-206.
24. Federal Emergency Management Agency, (2000). *Prestandard and commentary for the seismic rehabilitation of buildings*. FEMA 356, Washington, DC, 498 pp.
25. American Society of Civil Engineers (ASCE), (2000). *Prestandard and commentary for the seismic rehabilitation of buildings, prepared for the SAC joint venture*. Published by the Federal Emergency Management Agency, FEMA-356, Washington D.C.